3364–3372 *Nucleic Acids Research, 2016, Vol. 44, No. 7* *Published online 08 February 2016*
doi: 10.1093/nar/gkw069

Expression of multiple *Bacillus subtilis* genes is controlled by decay of *slrA* mRNA from Rho-dependent 3′ ends

Bo Liu[1], Daniel B. Kearns[2] and David H. Bechhofer[1,*]

[1]Department of Pharmacology and Systems Therapeutics, Box 1603, Icahn School of Medicine at Mount Sinai, New York, NY 10029, USA and [2]Department of Biology, Indiana University, Bloomington, IN 47405, USA

Received December 15, 2015; Revised January 27, 2016; Accepted January 28, 2016

ABSTRACT

Timely turnover of RNA is an important element in the control of bacterial gene expression, but relatively few specific targets of RNA turnover regulation are known. Deletion of the *Bacillus subtilis pnpA* gene, encoding the major 3′ exonuclease turnover enzyme, polynucleotide phosphorylase (PNPase), was shown previously to cause a motility defect correlated with a reduced level of the 32-gene *fla/che* flagellar biosynthesis operon transcript. *fla/che* operon transcript abundance has been shown to be inhibited by an excess of the small regulatory protein, SlrA, and here we find that *slrA* mRNA accumulated in the *pnpA*-deletion mutant. Mutation of *slrA* was epistatic to mutation of *pnpA* for the motility-related phenotype. Further, Rho-dependent termination was required for PNPase turnover of *slrA* mRNA. When the *slrA* gene was provided with a Rho-independent transcription terminator, gene regulation was no longer PNPase-dependent. Thus we show that the *slrA* transcript is a direct target of PNPase and that regulation of RNA turnover is a major determinant of motility gene expression. The interplay of specific transcription termination and mRNA decay mechanisms suggests selection for fine-tuning of gene expression.

INTRODUCTION

Levels of bacterial gene expression depend on the rate of transcription initiation, translation initiation, as well as the rate of messenger RNA decay. In *Bacillus subtilis* — the best-studied Gram-positive species in terms of mRNA turnover — initiation of mRNA decay is thought to begin most often with endonucleolytic cleavage catalyzed by RNase Y (1–3). Intra-transcript cleavage generates an upstream fragment that is degraded by polynucleotide phosphorylase (PNPase) or another 3′ exonuclease (4), and a downstream fragment that is subject to additional RNase Y-mediated cleavages or processive decay by RNase J1, a 5′ exonuclease (5,6). Decay from a transcript's 5′ end can also occur by the action of RNase J1, provided the 5′-triphosphorylated end has been converted to a monophosphorylated form by an RNA pyrophosphohydrolase (7). Exonucleolytic decay from a transcript's 3′ end is normally hindered by the strong secondary structure that is part of the Rho-independent transcription termination mechanism. Rho-dependent termination, which could generate 3′ ends without this strong structure, is not thought to play a significant role in *B. subtilis* transcription termination (8). Unlike in *Escherichia coli*, where about half of the transcription terminators are Rho-dependent and the *rho* gene is essential (9), the *B. subtilis rho* gene is not essential (10).

Biochemical evidence suggests that PNPase is the major mRNA turnover enzyme in *B. subtilis* (11,12). A strain that is deleted for the gene encoding PNPase, the Δ*pnpA* strain, shows several interesting phenotypes, including growth as non-motile chains of cells in liquid culture, competence deficiency and tetracycline sensitivity (12,13). However, at least in laboratory conditions, the Δ*pnpA* strain grows only slightly slower than the wild-type, perhaps suggesting that other exonuclease activities compensate in the mRNA turnover process when PNPase is absent. A recent RNA-Seq study analyzed the pattern of decay intermediates in *B. subtilis* strains that were either wild-type or deleted for the PNPase gene, and found altered levels for many mRNAs in the Δ*pnpA* strain (14). While many of the changes in gene expression in the Δ*pnpA* strain are likely due to indirect effects, a direct effect of the lack of PNPase was observed for about 10% of expressed genes, for which there was a significant increase in the level of 5′-proximal reads relative to the level of 3′-proximal reads.

Based on data from the RNA-Seq study, we were able to explain the chain growth phenotype of the Δ*pnpA* strain by an effect on the *fla/che* operon, a 27-kb operon containing 32 genes, of which the Sigma D transcription factor gene is the penultimate gene. RNA-Seq analysis revealed a 2-4-fold decrease in *fla/che* operon read levels overall, with a 3-fold decrease in *sigD* expression. This, in turn, caused depression

*To whom correspondence should be addressed. Tel: +1 212 241 5628; Fax: +1 212 996 7214; Email: david.bechhofer@mssm.edu

of the *sigD* regulon, including the autolysis genes that are required for separation of daughter cells upon cell division (15,16).

We have now examined the ultimate cause of decreased *fla/che* operon expression in the Δ*pnpA* strain. An earlier report demonstrated that *fla/che* operon RNA levels are controlled by SlrA, a small, 52-amino-acid protein. Insertion in the chromosome of a single extra copy of the *slrA* gene caused a severe decrease in expression of the *fla/che* operon (17). The effect was shown to be at a post-transcriptional level, although the mechanism remains undetermined. Here, we show that the level of *slrA* mRNA increases in the absence of PNPase, resulting in *slrA* overexpression, as evidenced by chain growth.

MATERIALS AND METHODS

Bacterial strains

The wild-type strain, BG1, is a *trpC2 thr-5* derivative of *B. subtilis* strain 168. BG546, the Δ*pnpA* strain, was described previously (14). For cell chaining assays, derivatives of the NCIB3610 strain ('3610') were constructed by SPP1 phage transduction. The Δ*slrA* and (*slrA*$^+$) strains were described previously (17). For construction of the P_{spac}-*slrA* allele, the *slrA* transcription unit, from 167 bp upstream of the CDS to 383 bp downstream of the coding sequence (CDS), was amplified with primers containing HindIII and SalI restriction endonuclease sites and cloned downstream of the P_{spac} promoter in plasmid pDR66 (18), giving pBL24. (The sequences of oligonucleotides used in this study are provided in Supplementary Table S1.) pBL24 DNA was linearized with restriction endonuclease NruI and used to transform the Δ*slrA* strain. The P_{slrA}-*lacZ* β-galactosidase reporter gene was constructed as follows: a polymerase chain reaction (PCR) product containing the P_{slrA} promoter was amplified from *B. subtilis* 3610 chromosomal DNA using the primers containing EcoRI and BamHI sites, and cloned into plasmid pDG268 (19), giving plasmid pDP422. pDP422 DNA was linearized with restriction endonuclease NruI for integration into the *amyE* locus.

The Δ*rho* strain, a kind gift of J. Helmann, was described previously (20), as was the Δ*rnr* strain (21). For construction of *slrATT*, complementary 41-mer oligonucleotides representing the *ermC* transcription terminator sequence were inserted 285 bp downstream of the *slrA* CDS in pBL24, according to a previously-described mutagenesis procedure (22).

Northern blotting

RNA was isolated from *B. subtilis* strains grown to mid-logarithmic phase in Luria-Bertani (LB) broth (10 g tryptone, 5 g yeast extract, 5 g NaCl per L), as described (23). RNA was fractionated either on a 1% denaturing agarose MOPS gel and blotted by wicking, or on a 6% denaturing polyacrylamide gel and electroblotted. 5′-end-labeled oligonucleotides were used as probes. The *slrA* probe was complementary to nts 88-119 of the *slrA* CDS. For P_{spac}-*slrA* transcripts, the probe was complementary to nts 1-27 of the *lacO* sequence. To control for RNA loading in Northern blot analyses, membranes were stripped and probed for 5S rRNA as described (24) or 16S rRNA using an oligonucleotide complementary to nts 1405–1424 (25). To determine the half-life of full-length RNA, exponential regression analysis ($R^2 > 0.9$) was performed on percentage of RNA remaining versus time. Since decay intermediates are being degraded and simultaneously generated from decay of full-length RNA, the half-life of decay intermediates was corrected based on an approach described previously (26).

3′-RACE

The 3′-RACE protocol was a slight modification of a published method (27). Total RNA from *pnpA*$^+$ and Δ*pnpA* strains was isolated as described above. 3′ ends were ligated to pre-adenylated linker (5′-rAppCTGTAGGCACCATCAAT-ddC-3′) by incubation for 2 h at 25°C with truncated T4 RNA ligase 2 (New England BioLabs). The ligated RNA was purified with RNeasy MinElute Cleanup Kit (Qiagen), and the 3′-proximal *slrA* sequence was amplified by using QIAGEN OneStep RT-PCR Kit with a primer complementary to the 3′ linker and a primer consisting of *slrA* CDS nts 34-59. PCR products were separated on a 1.5% agarose gel and appropriately-sized bands were excised and cloned into pGEM-T (Promega). For the band from the *pnpA*$^+$ strain, six clones were sequenced; for the band from the Δ*pnpA* strain, 12 clones were sequenced.

Phenotype assays

Overnight growth in tetracycline was performed as described (12). Competence was measured by a standard transformation protocol (28), using 1 μg of plasmid pYH250 DNA (24) or 1 μg of chromosomal DNA from a strain that had a chloramphenicol-resistance marker in the *amyE* locus, and selection for colonies resistant to 4 μg/ml chloramphenicol. Assay of β-galactosidase activity was as described previously (29).

Microscopy

Cells were grown in LB broth to 1 OD_{600}. Isopropyl β-D-thiogalactopyranoside (IPTG, Sigma) was added to the medium at the indicated concentration when appropriate. Phase-contrast microscopy was performed with a Nikon 80i microscope, using a phase-contrast objective Nikon Plan Apo 100×. Images were captured with a Photometrics Coolsnap HQ2 camera and Metamorph image software.

RESULTS

Absence of PNPase affects *slrA* mRNA levels, causing cell chaining

An RNA-Seq analysis of mRNA levels in wild-type and Δ*pnpA* strains showed decreased levels of *fla/che* operon mRNA in the strain lacking PNPase (14). As it had been shown earlier that an increased SlrA level correlates with reduced *fla/che* operon transcript abundance (17), we examined the RNA-Seq data for the *slrA* transcription unit (Figure 1A). Although the *slrA* CDS is only 156 nts, the RNA-Seq read data suggested that the transcription unit is about

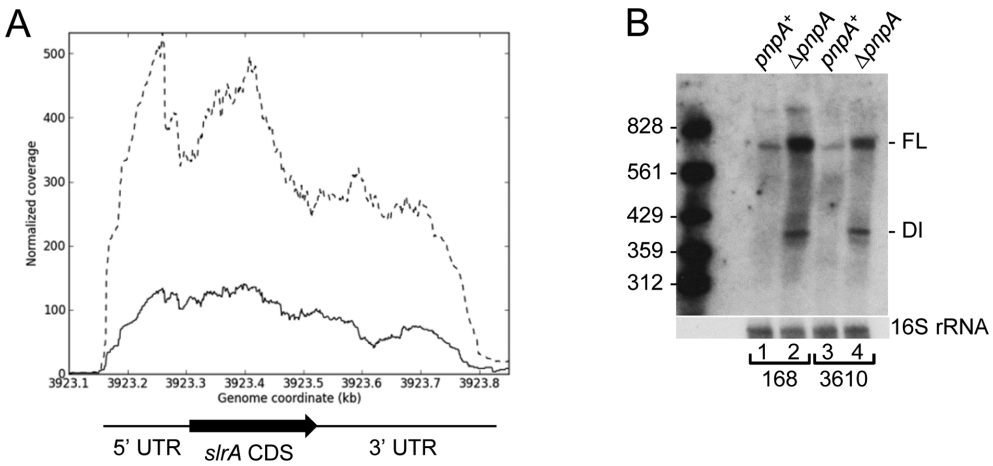

Figure 1. Increased level of *slrA* mRNA in the absence of PNPase. (**A**) Read data from RNA-Seq analysis of the *slrA* gene in *pnpA*$^+$ (solid line) and Δ*pnpA* (dashed line) strains. Genome coordinates on the X-axis; normalized reads on the Y-axis. Regions of the *slrA* transcription unit are indicated below the data. (**B**) Northern blot analysis of *slrA* mRNA in *Bacillus subtilis* 168 and 3610 backgrounds. Ten microgram of total RNA was fractionated on a 6% denaturing polyacrylamide gel. FL, full-length mRNA; DI, decay intermediate. Marker lane contained 5′-end-labeled fragments of a TaqI digest of plasmid pSE420 (51).

600 nts, with ∼170-nt 5′ untranslated region (UTR) and ∼330-nt 3′ UTR. The results in Figure 1A showed that *slrA* read levels were significantly elevated in the Δ*pnpA* strain, with a 3-4-fold read increase in the part of the transcription unit that includes the CDS, and a smaller increase in reads in the 3′-terminal half. The RNA-seq results were confirmed by Northern blot analysis, using an oligonucleotide probe complementary to a sequence 40 nts from the end of the *slrA* CDS. We observed ∼3.3-fold increase in the steady-state amount of full-length *slrA* mRNA in the Δ*pnpA* strain (average of two independent experiments), as well as an accumulation of decay intermediates, which were long enough to contain the complete *slrA* CDS (Figure 1B, lanes 1 and 2). Similar results were obtained in the *B. subtilis* 3610 strain (Figure 1B, lanes 3 and 4), which was used to assay chaining during cell growth (see below). We hypothesized that turnover of *slrA* mRNA by PNPase affects *fla/che* operon expression and *sigD* regulon expression.

As reported previously, depression of *fla/che* operon expression in the Δ*pnpA* mutant, and specifically the 3-fold decrease in *sigD* expression, was able to explain the chaining phenotype of the Δ*pnpA* mutant (14). If the effect of the loss of PNPase was due to elevated *slrA* mRNA, then deletion of the *slrA* gene should alleviate this effect. We used a previously-constructed Δ*slrA* strain (17) as well as a newly-constructed double deletion Δ*pnpA* Δ*slrA* strain to assay the chaining phenotype. Phase contrast microscopy of logarithmic phase cultures (Figure 2A) showed mostly dividing cells and a few short chains for the *pnpA*$^+$ strain, while there was extensive chaining in the '(*slrA*$^+$)' strain, which contains an additional chromosomal copy of the *slrA* gene (17). Similar extensive chaining was observed in the Δ*pnpA* strain, but deletion of the *pnpA* gene did not lead to chaining when the *slrA* gene was also deleted (Figure 2A; Δ*pnpA* Δ*slrA* strain). Thus, mutation of *slrA* was epistatic to mutation of *pnpA* for the cell-chaining phenotype.

Two other phenotypes reported for the Δ*pnpA* strain are competence deficiency (13) and tetracycline sensitivity (12). We tested whether *slrA* was epistatic to *pnpA* for these phenotypes as well. The data for overnight growth in the presence of tetracycline, shown in Figure 2B, indicated no significant difference in tetracycline sensitivity between the Δ*pnpA* and Δ*pnpA* Δ*slrA* strains. Thus, *slrA* was not epistatic to *pnpA* for tetracycline sensitivity. On the other hand, the data for competence indicated a partial suppression of the competence deficiency by deletion of *slrA* (Table 1). For chromosomal and plasmid DNA transformation, the Δ*pnpA* Δ*slrA* strain showed 9.8- and 2.7-fold, respectively, higher competence than the Δ*pnpA* strain (see 'Discussion' section).

The effect of PNPase on *slrA* mRNA is post-transcriptional

We determined whether the effect of PNPase on *slrA* mRNA was at the transcriptional or post-transcriptional level. First, Northern blot analysis of *lacZ* mRNA transcribed from the *slrA* promoter showed no difference in *lacZ* mRNA levels in the presence or absence of PNPase (data not shown). Assay of β-galactosidase expression from the P_{slrA}-*lacZ* construct also showed no significant difference in the presence or absence of PNPase (Table 2). To facilitate analysis of *slrA* mRNA, which is present at low levels when expressed from the wild-type allele, we constructed a Δ*slrA* strain that contained a wild-type copy of *slrA* under control of the IPTG-inducible P_{spac} promoter integrated at the *amyE* locus. Phenotypes associated with deletion of *pnpA* were the same for the P_{spac}-*slrA* strain as for strains with native *slrA* (data not shown). The effect of the *pnpA* deletion on accumulation of *slrA* mRNA was recapitulated with the P_{spac}-*slrA* construct (Figure 3A), where the amount of full-length *slrA* mRNA was 2.4-fold higher in the Δ*pnpA* strain than in the *pnpA*$^+$ strain, and a similar pattern of decay intermediates was observed. *slrA* mRNA half-life was measured in the presence of rifampin, and the results showed ∼2-fold increase in the half-life of full-length *slrA* mRNA in the absence of PNPase (Figure 3B, band 1), as well as in-

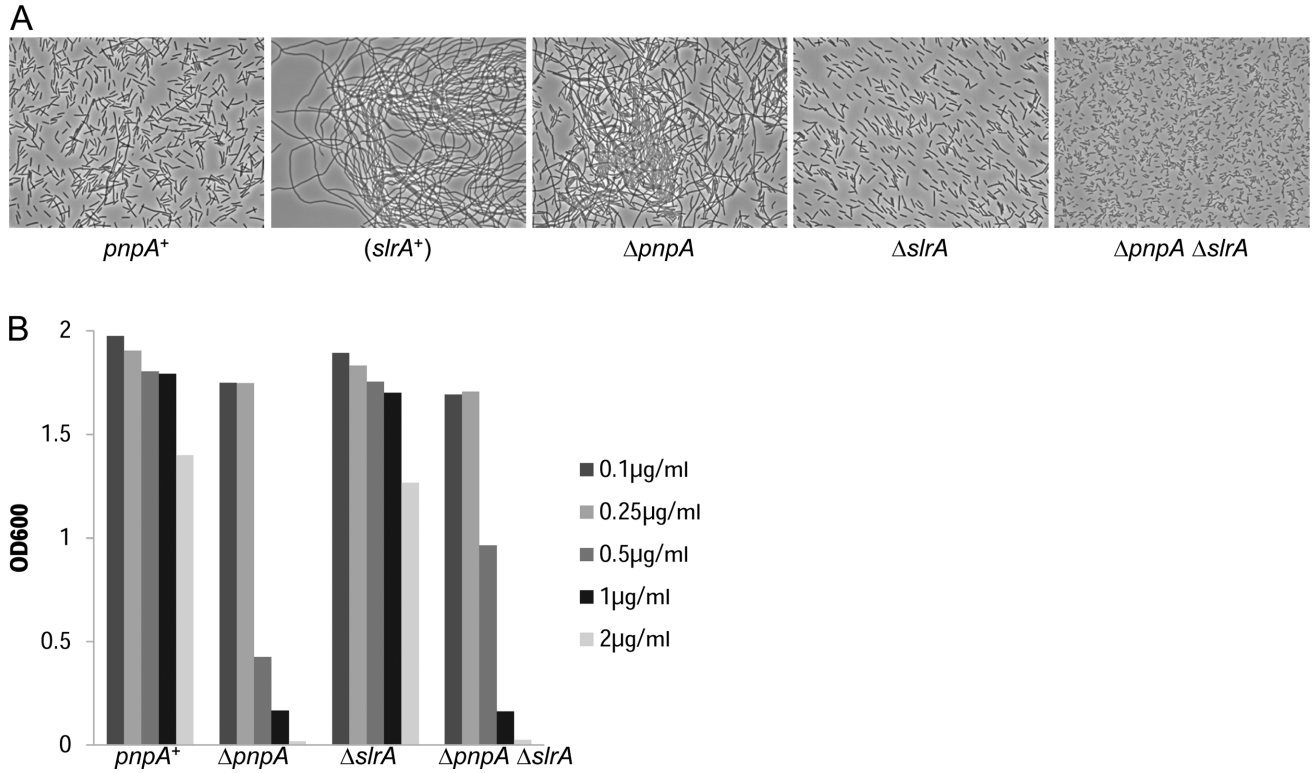

Figure 2. *slrA* mutation is epistatic to *pnpA* mutation for cell chaining. (**A**) Phase-contrast microscopy of cell chaining for the indicated strains. *pnpA*$^+$, wild-type 3610 strain; *slrA*$^+$, additional copy of *slrA* gene; Δ*pnpA*, deletion of gene encoding PNPase; Δ*slrA*, deletion of gene encoding SlrA; Δ*pnpA* Δ*slrA*, deletion of genes encoding PNPase and SlrA. (**B**) Overnight growth of strains in the presence of increasing concentrations of tetracycline.

Table 1. Percent transformants in Δ*pnpA* strains relative to *pnpA*$^+$ strain[a]

Strains	Chromosomal DNA	Plasmid DNA
Δ*pnpA*/*pnpA*$^+$	1.1 (1.1, 1.1)	9.0 (8.0, 10.0)
Δ*pnpA* Δ*slrA*/*pnpA*$^+$ Δ*slrA*	10.8 (10.4, 11.1)	24.4 (27.8, 21.0)

[a]Values are average of two independent experiments. Results from the two independent experiments are shown in parentheses.

Table 2. *lacZ* expression driven by *slrA* promoter

Strain	β-galactosidase activity per mg protein[a]
pnpA$^+$	241 ± 16
Δ*pnpA*	232 ± 10

[a]Mean ± standard deviation of three experiments.

creased half-life for two prominent decay intermediates that contain the *slrA* CDS (Figure 3B, bands 3 and 4).

slrA expression from the P_{spac} promoter afforded the opportunity to demonstrate conclusively that the effect of PNPase was not at the level of transcription from the *slrA* promoter. The chaining phenotype of *pnpA*$^+$ and Δ*pnpA* strains was assayed in the presence of increasing concentrations of IPTG. As can be seen in Figure 3C, no chaining was evident in either strain in the absence of IPTG. For the *pnpA*$^+$ strain, short chains and dividing cells were observed in the presence of 0.01 and 0.03 mM IPTG, while full chaining was observed when 0.10 mM IPTG was present. In the Δ*pnpA* strain, on the other hand, full chaining was observed even in the presence of 0.01 mM IPTG. These results confirmed that the chain growth that is observed in the absence of PNPase was the result of changes in *slrA* mRNA levels, independent of transcription from the *slrA* promoter.

Rho-dependent *slrA* mRNA 3′ ends

A previous analysis of *rpsO* mRNA decay in *B. subtilis* suggested that decay is unlikely to initiate from a 3′ end that is formed by Rho-independent transcription termination (30). Furthermore, *in vitro* experiments with purified PNPase showed that this enzyme is unable to degrade through the strong secondary structure of a Rho-independent transcription terminator (31). To address how PNPase could be controlling the full-length *slrA* mRNA half-life, we first used 3′ RACE to map the 3′ ends of *slrA* mRNA in the *pnpA*$^+$ and Δ*pnpA* strains. In the *pnpA*$^+$ strain, a single 3′ end was mapped at 301 nt downstream of the *slrA* stop codon (Figure 4A, open arrow). In the Δ*pnpA* strain, on the other hand, multiple 3′ ends were mapped, ranging from 301 to 333 nts downstream of the *slrA* stop codon (Figure 4A, short arrows). Immediately upstream of the 301-nt 3′ end is a predicted stem-loop structure that has a ΔG_0 value

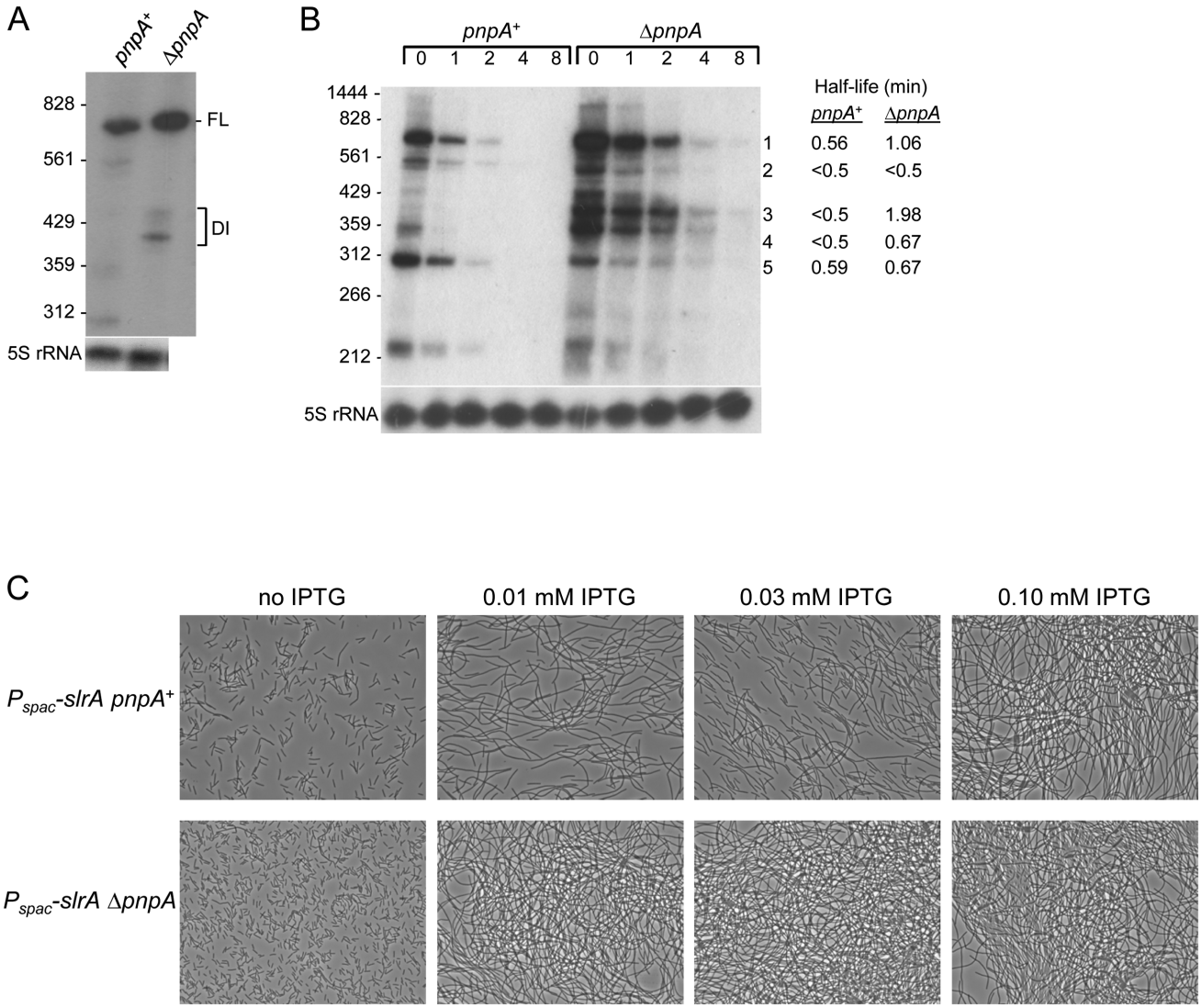

Figure 3. IPTG-induced *slrA* expression. (**A**) Northern blot analysis of *slrA* mRNA transcribed from the P_{spac} promoter. Ten microgram of total RNA was fractionated on a 6% denaturing polyacrylamide gel. Migration of 5′-end-labeled fragments of TaqI-digested pSE420 indicated at left. (**B**) Northern blot analysis of *slrA* mRNA half-life. Above each lane is time (min) after rifampin addition. Measured half-lives (average of two experiments) of specific bands are indicated on the right. Bands 1–4 are large enough to include the full *slrA* CDS. (**C**) Phase-contrast microscopy of cell chaining with increasing IPTG concentrations.

of −18 kcal/mol. The predicted structure is not typical of *B. subtilis* Rho-independent transcription terminators, almost all of which have completely base-paired, shorter stems (5-12 bp) followed by a 15-nt sequence containing 7–10 U residues (32). We therefore hypothesized that *slrA* transcription termination might be Rho-dependent. Northern blot analysis of P_{spac}-*slrA* RNAs in *rho*$^+$ and Δ*rho* strains is shown in Figure 4B. The absence of Rho resulted in a decreased intensity of the full-length band in the *pnpA*$^+$ and Δ*pnpA* backgrounds, as well as the appearance of higher molecular-weight RNA that is suggestive of transcriptional read-through (Figure 4B, lanes 3 and 4). Together, these results indicated that *slrA* transcription termination is Rho-dependent and terminates at multiple sites downstream of the stem-loop structure shown in Figure 4A. In the *pnpA*$^+$ strain, PNPase degrades *slrA* mRNA from these 3′ ends, although there is a partial block to PNPase processivity 5 nts from the edge of the stem-loop structure (nt 301). In the Δ*pnpA* strain, *slrA* mRNAs with various 3′ ends are not efficiently degraded and they accumulate, resulting in an increase in 'full-length' *slrA* mRNA, which is actually a collection of mRNAs of different sizes due to slightly different termination sites. Indeed, higher resolution Northern blot analysis showed several, closely-spaced 'full-length' *slrA* mRNA bands in the Δ*pnpA* strain that were larger than in the *pnpA*$^+$ strain (Figure 4D, lanes 1 and 2).

We asked whether the unusually long 5′ and 3′ UTRs of *slrA* mRNA were relevant to PNPase-mediated decay. Deletion constructs were made in the *slrA* 5′ UTR (Δ1 and Δ2) and 3′ UTR (Δ3), as shown in Figure 4C. Northern blot analysis of a higher resolution gel (Figure 4D) showed for all constructs the presence of a single full-length band in the *pnpA*$^+$ strain, which was the predicted length based on the size of the deletion, and additional bands of slightly larger

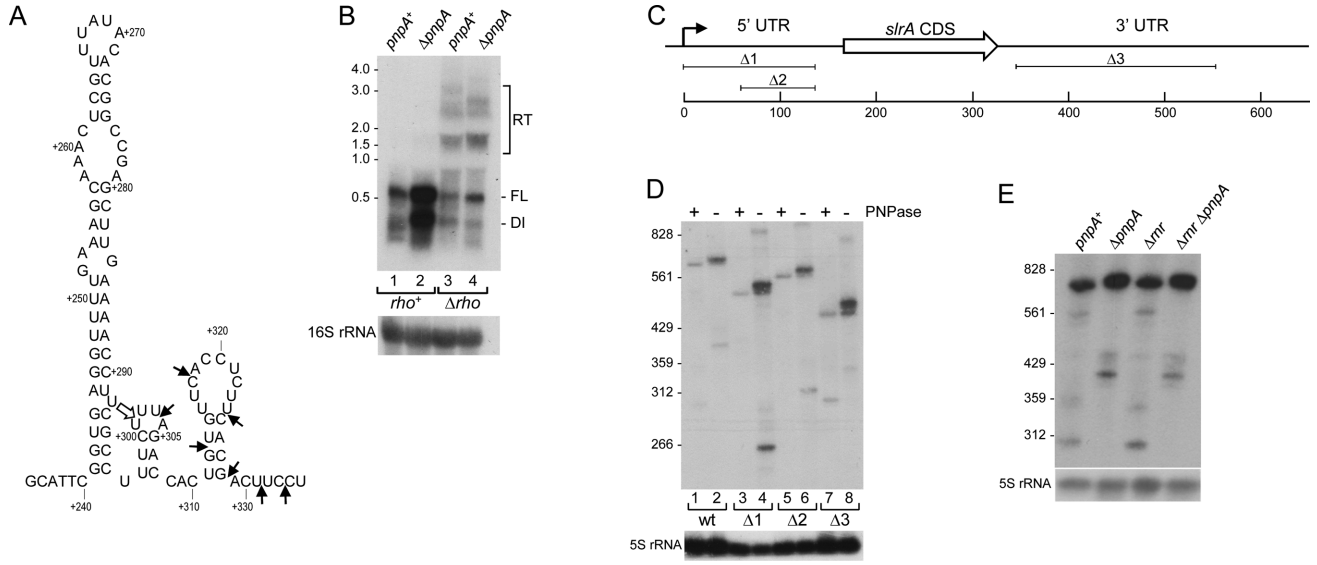

Figure 4. Rho-dependent termination of *slrA* transcription. (**A**) Sequence and predicted secondary structure (52) of 3′-proximal region of *slrA* 3′ UTR. Open arrow indicates location of major 3′ end at nt 301, mapped by 3′ RACE in the *pnpA*$^+$ strain. Location of additional 3′ ends mapped in the Δ*pnpA* strain indicated by short arrows. Numbering is from downstream of the *slrA* CDS. (**B**) Northern blot analysis of *slrA* mRNA in *rho*$^+$ and Δ*rho* strains. Ten microgram of total RNA was fractionated on a 1.0% MOPS-formaldehye agarose gel. RT, read-through. Migration of unlabeled RNA size markers indicated at left. (**C**) *slrA* gene schematic and location of *slrA* deletion constructs. Scale below is in base-pairs. (**D**) Northern blot analysis of P_{spac}-driven *slrA* mRNA from wild-type *slrA* gene and from deletion constructs. Ten microgram of total RNA was fractionated on a 6% denaturing polyacrylamide gel. (**E**) Northern blot analysis of *slrA* mRNA in the presence and absence of RNase R. Ten microgram of total RNA was fractionated on a 6% denaturing polyacrylamide gel.

size in the Δ*pnpA* strain. Furthermore, a higher level of *slrA* mRNA in the Δ*pnpA* background was observed for all deletion constructs. The data suggested that the 5′ and 3′ UTR sequences do not play a role in *slrA* mRNA decay.

We next tested whether the other known processive 3′ exonuclease of *B. subtilis*, RNase R, was involved in *slrA* mRNA turnover. Northern blot analysis of P_{spac}-*slrA* mRNA was performed in Δ*rnr* and Δ*rnr* Δ*pnpA* strains. As shown in Figure 4E, there was little difference in the steady-state patterns of *slrA* mRNA, with or without RNase R; full-length *slrA* mRNA accumulated in the absence of PNPase, whether or not RNase R was present. We conclude that primarily PNPase is responsible for efficient turnover from the 3′ ends of *slrA* mRNA generated by Rho-dependent transcription termination.

Rho-independent termination of *slrA* transcription phenocopies the Δ*pnpA* strain

To test the hypothesis that Rho-dependent termination of *slrA* transcription allows access to PNPase-mediated turnover from the 3′ end, a derivative of the P_{spac}-*slrA* construct was created that had a Rho-independent transcription terminator sequence inserted near the end of the 3′ UTR. The terminator was that of the *ermC* gene, which is predicted to form a strong secondary structure ($\Delta G_0 = -24.1$ kcal/mol) followed by five U residues (Figure 5A). The *slrA* gene with the *ermC* transcription terminator sequence is referred to as *slrATT*. The expectation was that the presence of 3′-terminal structure would block PNPase decay, and even in the *pnpA*$^+$ strain there would be an accumulation of *slrA* mRNA and inhibition of *fla/che* operon expression. Northern blot analysis showed that *slrATT* mRNA was detected as a single band in both *pnpA*$^+$ and Δ*pnpA* strains (Figure 5B). Importantly, *slrATT* mRNA was present at a higher level than *slrA* mRNA in the *pnpA*$^+$ strain (∼8-fold), and, unlike *slrA* mRNA that was terminated in a Rho-dependent manner, there was no difference in steady-state mRNA level between the *pnpA*$^+$ and Δ*pnpA* strains. These results suggested that *slrATT* mRNA was not a substrate for PNPase-mediated decay, which likely resulted in a higher level of SlrA protein. To show the effect of protecting *slrA* mRNA from decay, the chain growth phenotype of the P_{spac}-*slrATT* strain was tested. We showed above that when the P_{spac}-*slrA* strain was grown in the presence of 0.01 mM IPTG, there was limited chaining when PNPase was present and a high degree of chaining when PNPase was absent (Figure 3C). In contrast, the P_{spac}-*slrATT* strain showed massive chaining even when only 0.01 mM IPTG was added and PNPase was present (Figure 5C). Thus, Rho-mediated termination of *slrA* transcription, in concert with PNPase-mediated mRNA decay, is required to set a suitable level of *slrA* expression that allows motile *B. subtilis* growth.

DISCUSSION

The results presented here indicate that timely turnover of *slrA* mRNA is required for precise regulation of the *fla/che* operon (32 genes) and, indirectly, the rest of the *sigD* regulon (50 genes). Thus, the expression level of over 80 genes is determined by the ability of PNPase to degrade *slrA* mRNA and confer on it a relatively short half-life. PNPase-mediated decay of bacterial regulatory RNAs, such as small RNAs (sRNAs) and leader RNAs, has been documented previously: the decay (or stability) of a number of *E. coli*

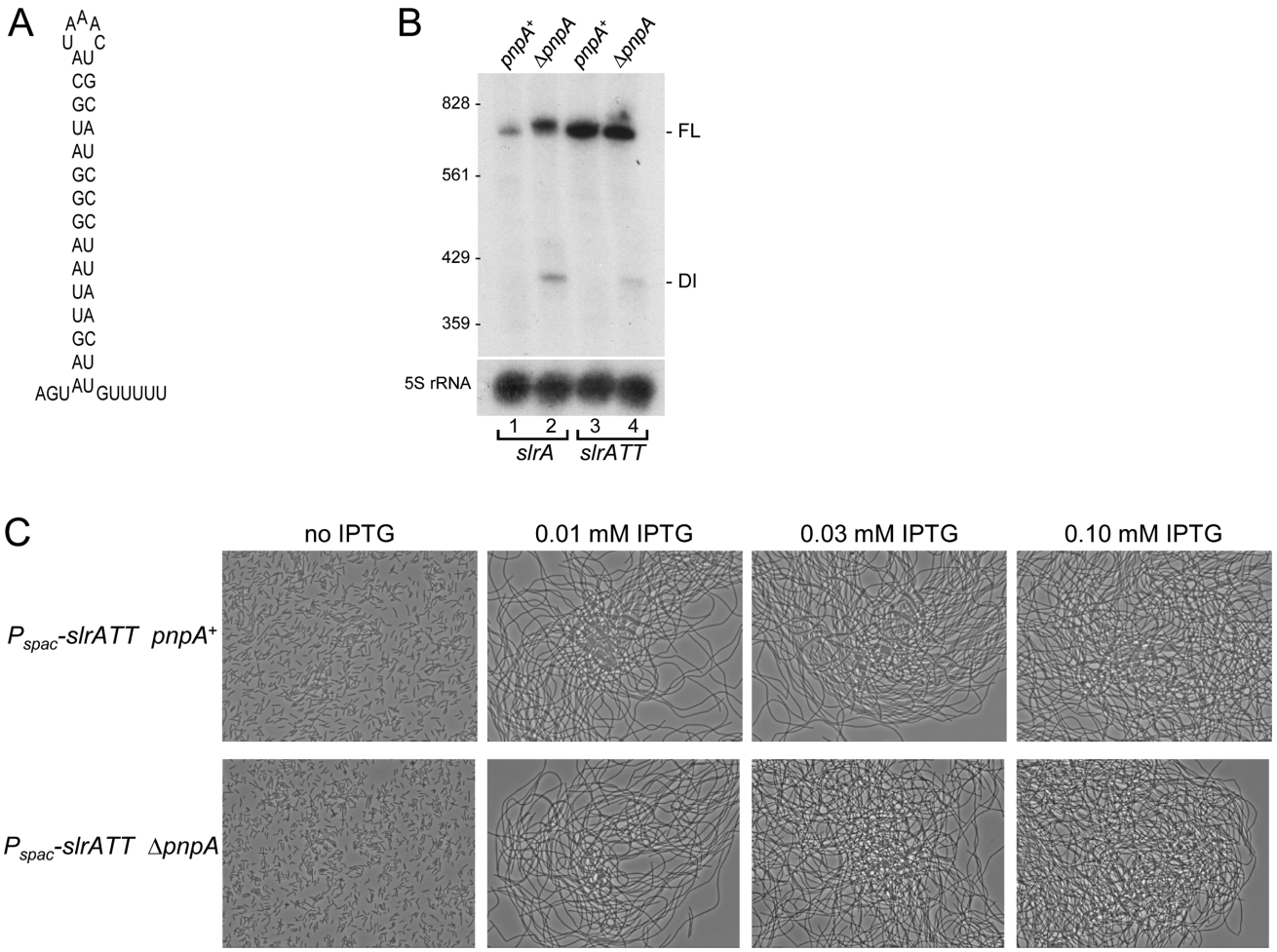

Figure 5. *slrA* with Rho-independent terminator. (**A**) Predicted secondary structure of the *ermC* transcription terminator. (**B**) Northern blot analysis of *slrA* mRNA carrying the *ermC* transcription terminator (*slrATT*). Ten microgram of total RNA was fractionated on a 6% denaturing polyacrylamide gel. (**C**) Phase-contrast microscopy of *slrATT* strains with increasing IPTG concentrations.

and *Salmonella typhimurium* sRNAs are regulated by PNPase (see (33) and references therein); control of *E. coli* C biofilm formation by PNPase is hypothesized to occur via degradation of small regulatory RNAs (34); autoregulation of the *E. coli pnp* gene relies on efficient degradation of the *pnp* leader region RNA by PNPase (35); and we have shown that regulation of *B. subtilis trp* operon gene expression requires efficient degradation of *trp* leader RNA by PNPase (36). However, we are not aware of another report in which PNPase-mediated decay of a full-length mRNA is crucial for the control of many genes.

We show here that *slrA* mRNA decay by PNPase depends on Rho-dependent transcription termination (Figures 4 and 5). A recent transcriptome analysis suggested that deletion of the *rho* gene causes extended transcription of many mRNAs (37), and, indeed, the *slrA* gene is one of these. However, only a few transcripts acted on by Rho have been examined in any detail: the *rho* gene itself (8), the *trp* operon (38), and, very recently, the *rplJL* operon (39). In these cases, Rho acts either in a leader region or in the first gene of an operon to terminate transcription before synthesis of protein coding sequences. For *slrA*, Rho apparently binds downstream of a coding region to cause transcription termination that leaves 3′ ends susceptible to PNPase decay. PNPase is unable to degrade strong stem-loop structures *in vitro* (31), and it is not known whether *in vivo* association with the RNA helicase CshA (40) allows it to degrade Rho-independent transcription terminator sequences. It is also not known whether an iterative polyadenylation process, which in *E. coli* is catalyzed by poly(A) polymerase and confers susceptibility of 3′-terminal RNA fragments to decay (41), exists in *B. subtilis*. Experiments to test this have not yet been possible, since the gene encoding a *B. subtilis* poly(A) polymerase remains elusive (42). Recent evidence in our laboratory suggests that 3′-terminal mRNA fragments are degraded for the most part by RNase J1 (our unpublished data). It is therefore assumed that initiation of decay for mRNAs with a Rho-independent terminator occurs either by endonucleolytic cleavage catalyzed by RNase Y, or by 5′-to-3′ exonuclease activity of RNase J1 acting on a 5′-monophosphate end (6). It is expected that only for mRNAs whose transcription termination is Rho-dependent could efficient decay occur by a 3′ exonuclease activity starting from a native 3′ end. Although *B. subtilis* contains at least

four 3′ exoribonucleases (4), in the case of *slrA* mRNA it appears that primarily PNPase engages in this degradative function (Figure 4E).

An interesting aspect of *slrA* mRNA is its unusually long 3′ UTR. A survey of the location of Rho-independent transcription terminators, relative to an upstream stop codon, determined that 93% occur within 100 bp of the stop codon, and many of the remaining terminators may be functioning in transcription termination of convergently transcribed genes (32). For *slrA*, termination occurs ∼330 nts downstream of the stop codon, and the next predicted gene is in the same orientation and starts 100 bp away. A 208-nt deletion starting 18 nts downstream of the *slrA* CDS (Δ3, Figure 4C) gave the same pattern of multiple 'full-length' *slrA* mRNA bands as the wild-type gene and as two deletions in the 5′ UTR (Figure 4D). The implication is that a Rho binding site exists in the remaining 75 nts of the Δ3 construct. For *E. coli*, the primary characteristics of Rho binding sites are ribosome-free, unstructured and C-rich (43). *B. subtilis* Rho has similar biochemical characteristics to *E. coli* Rho (8), suggesting that it will have similar requirements for binding. However, we were unable to recognize specific attributes of the 3′-proximal 75-nt sequence that would explain Rho binding. This sequence has an equal distribution of the four deoxyribonucleotides, and 56 nts of the sequence can be predicted to form a stable secondary structure (Figure 4A). The presence of a 'C > G bubble,' defined as a relatively C-rich and G-poor region over a length of 78 nts that precedes a Rho-dependent transcription termination site in many cases (44), was not observed in the corresponding region of the *slrA* gene (see Supplementary Figure S1). Clearly, there is much to be learned about the mechanism of *B. subtilis* Rho activity. Our discovery here of Rho-dependent transcription termination for a full-length mRNA, as well as the recent finding that the *rho* gene affects expression of genes involved in antibiotic resistance (20), should prompt additional study of the requirements for Rho activity in *B. subtilis*.

We showed that *slrA* was epistatic to *pnpA* for the chaining phenotype (Figure 2A). This, as well as chaining in the presence of increasing IPTG concentration for P_{spac}-promoted *slrA* (Figure 3C), are strong evidence for the hypothesis that the cause of the chaining in the absence of PNPase is due to a post-transcriptional effect on *slrA* expression. Two other phenotypes caused by the loss of PNPase did not appear to involve *slrA* mRNA. Tetracycline-sensitivity of the Δ*pnpA* strain, the basis of which is unknown, was not affected by the deletion of *slrA* (Figure 2B). Interestingly, competence deficiency of the Δ*pnpA* strain was partially suppressed by the *slrA* knockout (Table 1). Characterization of *com* gene expression in the Δ*pnpA* strain by Dubnau *et al*. suggested that loss of PNPase affected regulated expression of several competence genes, including *comG*, *comK* and *srfAA* (*comS*) (13). A simple explanation for the observed partial suppression in the Δ*slrA* strain is that the protein complex required for DNA uptake is located at the cell poles (45,46). Cells growing in long chains would have fewer poles available for presentation of transforming DNA to the DNA-binding apparatus. Alleviation of the chain growth by deletion of *slrA* may thus explain partial restoration of the competence defect caused by loss of PNPase.

The finding that efficient decay of an mRNA figures prominently in the regulation of a large number of genes supports the concept that models of gene expression networks must take into account not only transcriptional and translational control, but also control at the level of mRNA decay (47). In the case of *slrA*, the involvement of PNPase as a controlling factor relies on the generation of PNPase-susceptible 3′ ends by the action of Rho. *slrA* is not only required for *fla/che* operon regulation, but is part of a gene network that controls biofilm formation (48–50). Fine-tuning of *slrA* expression is likely necessary for its functions, and there has been selection for this control to involve an unusual form of mRNA decay. We expect that more examples of the interplay of Rho-dependent transcription termination and mRNA turnover will be discovered.

SUPPLEMENTARY DATA

Supplementary Data are available at NAR Online.

FUNDING

National Institutes of Health [GM-100137 to D.H.B., GM-093030 to D.B.K.]. Funding for open access charge: National Institutes of Health [GM-100137 D.H.B.].
Conflict of interest statement. None declared.

REFERENCES

1. Shahbabian,K., Jamalli,A., Zig,L. and Putzer,H. (2009) RNase Y, a novel endoribonuclease, initiates riboswitch turnover in Bacillus subtilis. *EMBO J.*, **28**, 3523–3533.
2. Lehnik-Habrink,M., Schaffer,M., Mader,U., Diethmaier,C., Herzberg,C. and Stulke,J. (2011) RNA processing in Bacillus subtilis: identification of targets of the essential RNase Y. *Mol. Microbiol.*, **81**, 1459–1473.
3. Durand,S., Gilet,L., Bessieres,P., Nicolas,P. and Condon,C. (2012) Three essential ribonucleases-RNase Y, J1, and III-control the abundance of a majority of Bacillus subtilis mRNAs. *PLoS Genet.*, **8**, e1002520.
4. Oussenko,I.A., Abe,T., Ujiie,H., Muto,A. and Bechhofer,D.H. (2005) Participation of 3′-to-5′ exoribonucleases in the turnover of Bacillus subtilis mRNA. *J. Bacteriol.*, **187**, 2758–2767.
5. Daou-Chabo,R., Mathy,N., Benard,L. and Condon,C. (2009) Ribosomes initiating translation of the hbs mRNA protect it from 5′-to-3′ exoribonucleolytic degradation by RNase J1. *Mol. Microbiol.*, **71**, 1538–1550.
6. Lehnik-Habrink,M., Lewis,R.J., Mader,U. and Stulke,J. (2012) RNA degradation in Bacillus subtilis: an interplay of essential endo- and exoribonucleases. *Mol. Microbiol.*, **84**, 1005–1017.
7. Richards,J., Liu,Q., Pellegrini,O., Celesnik,H., Yao,S., Bechhofer,D.H., Condon,C. and Belasco,J.G. (2011) An RNA pyrophosphohydrolase triggers 5′-exonucleolytic degradation of mRNA in Bacillus subtilis. *Mol. Cell*, **43**, 940–949.
8. Ingham,C.J., Dennis,J. and Furneaux,P.A. (1999) Autogenous regulation of transcription termination factor Rho and the requirement for Nus factors in Bacillus subtilis. *Mol. Microbiol.*, **31**, 651–663.
9. Ciampi,M.S. (2006) Rho-dependent terminators and transcription termination. *Microbiology*, **152**, 2515–2528.
10. Quirk,P.G., Dunkley,E.A. Jr, Lee,P. and Krulwich,T.A. (1993) Identification of a putative Bacillus subtilis rho gene. *J. Bacteriol.*, **175**, 647–654.
11. Deutscher,M.P. and Reuven,N.B. (1991) Enzymatic basis for hydrolytic versus phosphorolytic mRNA degradation in Escherichia

coli and Bacillus subtilis. *Proc. Natl. Acad. Sci. U.S.A.*, **88**, 3277–3280.
12. Wang,W. and Bechhofer,D.H. (1996) Properties of a Bacillus subtilis polynucleotide phosphorylase deletion strain. *J. Bacteriol.*, **178**, 2375–2382.
13. Luttinger,A., Hahn,J. and Dubnau,D. (1996) Polynucleotide phosphorylase is necessary for competence development in Bacillus subtilis. *Mol. Microbiol.*, **19**, 343–356.
14. Liu,B., Deikus,G., Bree,A., Durand,S., Kearns,D.B. and Bechhofer,D.H. (2014) Global analysis of mRNA decay intermediates in Bacillus subtilis wild-type and polynucleotide phosphorylase-deletion strains. *Mol. Microbiol.*, **94**, 41–55.
15. Marquez,L.M., Helmann,J.D., Ferrari,E., Parker,H.M., Ordal,G.W. and Chamberlin,M.J. (1990) Studies of sigma D-dependent functions in Bacillus subtilis. *J. Bacteriol.*, **172**, 3435–3443.
16. Chen,R., Guttenplan,S.B., Blair,K.M. and Kearns,D.B. (2009) Role of the sigmaD-dependent autolysins in Bacillus subtilis population heterogeneity. *J. Bacteriol.*, **191**, 5775–5784.
17. Cozy,L.M., Phillips,A.M., Calvo,R.A., Bate,A.R., Hsueh,Y.H., Bonneau,R., Eichenberger,P. and Kearns,D.B. (2012) SlrA/SinR/SlrR inhibits motility gene expression upstream of a hypersensitive and hysteretic switch at the level of sigma(D) in Bacillus subtilis. *Mol. Microbiol.*, **83**, 1210–1228.
18. Ireton,K., Rudner,D.Z., Siranosian,K.J. and Grossman,A.D. (1993) Integration of multiple developmental signals in Bacillus subtilis through the Spo0A transcription factor. *Genes Dev.*, **7**, 283–294.
19. Antoniewski,C., Savelli,B. and Stragier,P. (1990) The spoIIJ gene, which regulates early developmental steps in Bacillus subtilis, belongs to a class of environmentally responsive genes. *J. Bacteriol.*, **172**, 86–93.
20. Lee,Y.H. and Helmann,J.D. (2014) Mutations in the primary sigma factor sigmaA and termination factor rho that reduce susceptibility to cell wall antibiotics. *J. Bacteriol.*, **196**, 3700–3711.
21. Oussenko,I.A. and Bechhofer,D.H. (2000) The yvaJ gene of Bacillus subtilis encodes a 3′-to-5′ exoribonuclease and is not essential in a strain lacking polynucleotide phosphorylase. *J. Bacteriol.*, **182**, 2639–2642.
22. Wang,W. and Malcolm,B.A. (1999) Two-stage PCR protocol allowing introduction of multiple mutations, deletions and insertions using QuikChange Site-Directed Mutagenesis. *Biotechniques*, **26**, 680–682.
23. Bechhofer,D.H., Oussenko,I.A., Deikus,G., Yao,S., Mathy,N. and Condon,C. (2008) Analysis of mRNA decay in Bacillus subtilis. *Methods Enzymol.*, **447**, 259–276.
24. Sharp,J.S. and Bechhofer,D.H. (2003) Effect of translational signals on mRNA decay in Bacillus subtilis. *J. Bacteriol.*, **185**, 5372–5379.
25. Sulthana,S. and Deutscher,M.P. (2013) Multiple exoribonucleases catalyze maturation of the 3′ terminus of 16S ribosomal RNA (rRNA). *J. Biol. Chem.*, **288**, 12574–12579.
26. Ebbole,D.J. and Zalkin,H. (1988) Detection of pur operon-attenuated mRNA and accumulated degradation intermediates in Bacillus subtilis. *J. Biol. Chem.*, **263**, 10894–10902.
27. Zhang,J. and Olsen,G.J. (2009) Messenger RNA processing in Methanocaldococcus (Methanococcus) jannaschii. *RNA*, **15**, 1909–1916.
28. Dubnau,D. and Davidoff-Abelson,R. (1971) Fate of transforming DNA following uptake by competent Bacillus subtilis. I. Formation and properties of the donor-recipient complex. *J. Mol. Biol.*, **56**, 209–221.
29. Dubnau,D. (1985) Induction of ermC requires translation of the leader peptide. *EMBO J.*, **4**, 533–537.
30. Yao,S. and Bechhofer,D.H. (2010) Initiation of decay of Bacillus subtilis rpsO mRNA by endoribonuclease RNase Y. *J. Bacteriol.*, **192**, 3279–3286.
31. Deikus,G. and Bechhofer,D.H. (2007) Initiation of decay of Bacillus subtilis trp leader RNA. *J. Biol. Chem.*, **282**, 20238–20244.
32. de Hoon,M.J., Makita,Y., Nakai,K. and Miyano,S. (2005) Prediction of transcriptional terminators in Bacillus subtilis and related species. *PLoS Comput. Biol.*, **1**, e25.
33. Saramago,M., Barria,C., Dos Santos,R.F., Silva,I.J., Pobre,V., Domingues,S., Andrade,J.M., Viegas,S.C. and Arraiano,C.M. (2014) The role of RNases in the regulation of small RNAs. *Curr. Opin. Microbiol.*, **18**, 105–115.
34. Carzaniga,T., Antoniani,D., Deho,G., Briani,F. and Landini,P. (2012) The RNA processing enzyme polynucleotide phosphorylase negatively controls biofilm formation by repressing poly-N-acetylglucosamine (PNAG) production in Escherichia coli C. *BMC Microbiol.*, **12**, 270–281.
35. Jarrige,A.C., Mathy,N. and Portier,C. (2001) PNPase autocontrols its expression by degrading a double-stranded structure in the pnp mRNA leader. *EMBO J.*, **20**, 6845–6855.
36. Deikus,G., Babitzke,P. and Bechhofer,D.H. (2004) Recycling of a regulatory protein by degradation of the RNA to which it binds. *Proc. Natl. Acad. Sci. U.S.A.*, **101**, 2747–2751.
37. Nicolas,P., Mader,U., Dervyn,E., Rochat,T., Leduc,A., Pigeonneau,N., Bidnenko,E., Marchadier,E., Hoebeke,M., Aymerich,S. *et al.* (2012) Condition-dependent transcriptome reveals high-level regulatory architecture in Bacillus subtilis. *Science*, **335**, 1103–1106.
38. Yakhnin,H., Babiarz,J.E., Yakhnin,A.V. and Babitzke,P. (2001) Expression of the Bacillus subtilis trpEDCFBA operon is influenced by translational coupling and Rho termination factor. *J. Bacteriol.*, **183**, 5918–5926.
39. Yakhnin,H., Yakhnin,A.V. and Babitzke,P. (2015) Ribosomal protein L10(L12)4 autoregulates expression of the Bacillus subtilis rplJL operon by a transcription attenuation mechanism. *Nucleic Acids Res.*, **43**, 7032–7043.
40. Lehnik-Habrink,M., Pfortner,H., Rempeters,L., Pietack,N., Herzberg,C. and Stulke,J. (2010) The RNA degradosome in Bacillus subtilis: identification of CshA as the major RNA helicase in the multiprotein complex. *Mol. Microbiol.*, **77**, 958–971.
41. Regnier,P. and Hajnsdorf,E. (2009) Poly(A)-assisted RNA decay and modulators of RNA stability. *Prog. Mol. Biol. Transl. Sci.*, **85**, 137–185.
42. Campos-Guillen,J., Bralley,P., Jones,G.H., Bechhofer,D.H. and Olmedo-Alvarez,G. (2005) Addition of poly(A) and heteropolymeric 3′ ends in Bacillus subtilis wild-type and polynucleotide phosphorylase-deficient strains. *J. Bacteriol.*, **187**, 4698–4706.
43. Richardson,J.P. (2003) Loading Rho to terminate transcription. *Cell*, **114**, 157–159.
44. Alifano,P., Rivellini,F., Limauro,D., Bruni,C.B. and Carlomagno,M.S. (1991) A consensus motif common to all Rho-dependent prokaryotic transcription terminators. *Cell*, **64**, 553–563.
45. Hahn,J., Maier,B., Haijema,B.J., Sheetz,M. and Dubnau,D. (2005) Transformation proteins and DNA uptake localize to the cell poles in Bacillus subtilis. *Cell*, **122**, 59–71.
46. Kidane,D. and Graumann,P.L. (2005) Intracellular protein and DNA dynamics in competent Bacillus subtilis cells. *Cell*, **122**, 73–84.
47. Silva,I.J., Saramago,M., Dressaire,C., Domingues,S., Viegas,S.C. and Arraiano,C.M. (2011) Importance and key events of prokaryotic RNA decay: the ultimate fate of an RNA molecule. *Wiley Interdiscip. Rev. RNA*, **2**, 818–836.
48. Kobayashi,K. (2008) SlrR/SlrA controls the initiation of biofilm formation in Bacillus subtilis. *Mol. Microbiol.*, **69**, 1399–1410.
49. Chai,Y., Kolter,R. and Losick,R. (2009) Paralogous antirepressors acting on the master regulator for biofilm formation in Bacillus subtilis. *Mol. Microbiol.*, **74**, 876–887.
50. Newman,J.A. and Lewis,R.J. (2013) Exploring the role of SlrR and SlrA in the SinR epigenetic switch. *Commun. Integr. Biol.*, **6**, e25658.
51. Brosius,J. (1992) Compilation of superlinker vectors. *Meth. Enzymol.*, **216**, 469–483.
52. Zuker,M. (2003) Mfold web server for nucleic acid folding and hybridization prediction. *Nucleic Acids Res.*, **31**, 3406–3415.